

## Bipolar thermoelectric superconducting single-electron transistor

Sebastiano Battisti,<sup>\*</sup> Giorgio De Simoni<sup>✉</sup>, Luca Chiroli<sup>✉</sup>, Alessandro Braggio,<sup>†</sup> and Francesco Giazotto<sup>✉‡</sup>  
*NEST, Istituto Nanoscienze-CNR and Scuola Normale Superiore, I-56127 Pisa, Italy*

 (Received 24 May 2023; accepted 22 November 2023; published 25 January 2024)

Thermoelectric effects in normal metals and superconductors are usually very small due to the presence of electron-hole symmetry. Here, we show that superconducting junctions brought out of equilibrium manifest a sizable bipolar thermoelectric effect that stems from a *strong* violation of the detailed balance determined by the crucial role of the interactions at the mean-field level. To fully control the effect, we consider a thermally biased *SIS'* junction where the capacitance of the central *S'* region is small enough to establish a Coulomb blockade regime. By exploiting charging effects we are able to tune the Seebeck voltage, the thermocurrent, and thereby the power output of this structure, via an external gate voltage. We then analyze the main figures of merit of bipolar thermoelectricity and we prospect for possible applications.

DOI: [10.1103/PhysRevResearch.6.L012022](https://doi.org/10.1103/PhysRevResearch.6.L012022)

**Introduction.** Thermal transport and quantum thermodynamics at the nanoscale have recently attracted a growing interest [1–19], thanks to the opportunity the thermoelectric effects offer in heat management and nanodevices energy efficiency [20–30]. In the linear regime thermoelectricity requires a breaking of the electron-hole (EH) symmetry at the scattering level, implying a nonreciprocal *IV* characteristic, i.e.,  $I(V, \Delta T) \neq -I(-V, \Delta T)$ , where  $\Delta T$  is the temperature difference. Metals, that are almost spectrally electron-hole (EH) symmetric, show nearly negligible Seebeck coefficients [31] and present zero thermovoltages in the superconducting phase. In the nonlinear regime it has been demonstrated [32,33] that an *SIS'* thermally biased superconducting tunnel junction, when the Josephson coupling is sufficiently suppressed, spontaneously develops a voltage bias: a manifestation of spontaneous breaking of the EH symmetry of the whole junction. The system exhibits a sizable thermopower, yielding an effective Seebeck coefficient (*S*) as large as  $\sim 10^5$  times its value in the normal state [34,35]. Crucially, the spectral EH symmetry determines a full *bipolar* effect, i.e., reciprocal *IV* characteristics, and we call this effect *bipolar thermoelectricity*. Notably, the effect emerges in *SIS'* structures when the temperature difference is of the order of the gaps and it nonlinearly depends on the gaps' asymmetry. Here, we investigate the nature of the spontaneous EH symmetry breaking so far highlighted in the nonlinear regime and demonstrate that its origin is found in the unique interacting behavior of the BCS density of states (DOS) as obtained in mean-field theory. We associate the bipolar thermoelectricity

to a *strong* violation of the detail balance of the tunneling rates, which is induced by the temperature difference in the junction, the gap asymmetry, the monotonous decreasing of the DOS, and the interacting nature of BCS theory. To harvest the effect, we consider an *SIS'* structure where a central superconducting (SC) island featuring strong Coulomb interaction is sandwiched between two SC leads via tunnel barriers. We exploit the gating properties of the Coulombic island to control the bipolar thermoelectric performances of the engine, showing that it substantially differs from standard thermoelectricity in quantum dots. This unique electrical tunability differs from other platforms [36] and can be relevant for energy harvesting in superconducting quantum processors and radiation sensors [37].

**Model.** The *SIS'* structure under investigation is shown in Fig. 1(a), and consists of two SC leads [*L,R*, red part in Fig. 1(a)] with the energy gap  $\Delta$  put in tunnel contact with a Coulombic island [central blue part in Fig. 1(a)] with a different gap  $\Delta_{\text{is}}$ , via two identical barriers of resistance  $R_{L/R}$ . To observe bipolar thermoelectricity the leads are chosen to have a larger gap than the island,  $\Delta > \Delta_{\text{is}}$ , and they are kept at a temperature of  $T_{\text{hot}} > T_{\text{cold}} \equiv T_{\text{is}} = 0.2 T_C$ , where  $T_C$  is the critical temperature of the leads. The tunneling barriers are assumed to be resistive enough to make the Josephson energy negligible with respect to thermal energy, allowing the Josephson coupling to be neglected [38]. Yet, in order to observe the Coulomb blockade we assume the charging energy of the island,  $E_C = e^2/2C_{\text{tot}}$ , with  $C_{\text{tot}}$  the total island capacitance, to be large enough that  $E_C \gg k_B T_l$ , with  $l = \text{is}, L, \text{ and } R$  and  $E_C \gtrsim \Delta$ .

For sufficiently resistive barriers the full transport properties of the system can be described through the rates  $\Gamma_j(\delta U)$ , with  $j = R$  and  $L$ , that describe the tunneling probability through the *j*th barrier by the Fermi golden rule [39,40]

$$\Gamma_j = \frac{1}{e^2 R_j} \int_{-\infty}^{\infty} dE n_{\text{is}}(E + \delta U) [1 - f_{\text{is}}(E + \delta U)] n_j(E) f_j(E), \quad (1)$$

<sup>\*</sup>sebastiano.battisti@sns.it

<sup>†</sup>alessandro.braggio@nano.cnr.it

<sup>‡</sup>francesco.giazotto@sns.it

Published by the American Physical Society under the terms of the [Creative Commons Attribution 4.0 International](https://creativecommons.org/licenses/by/4.0/) license. Further distribution of this work must maintain attribution to the author(s) and the published article's title, journal citation, and DOI.

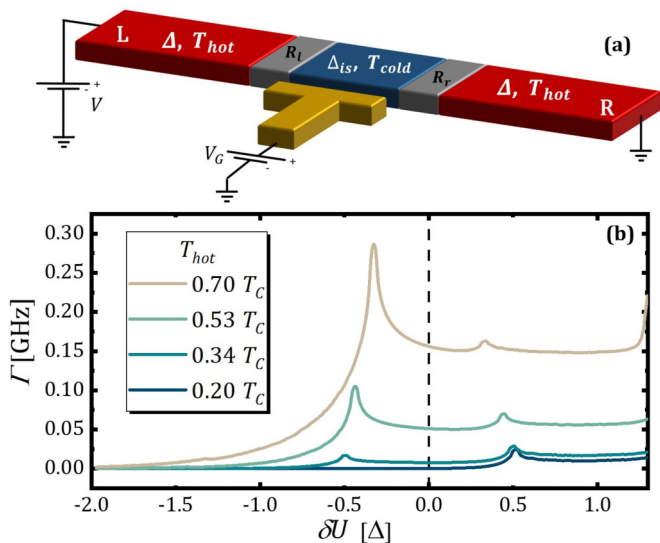


FIG. 1. (a) Scheme of the *SISIS* transistor. The red-colored parts show the hot superconductors and the blue-colored part shows the cold one.  $V$  and  $V_G$  denote the source-drain and gate voltages, respectively. (b) Tunneling rates vs energy for different values of  $T_{\text{hot}}$  at  $T_{\text{cold}} = 0.2 T_C$ .

where  $e$  is the electron charge;  $\delta U$  is the electrostatic energy acquired ( $\delta U > 0$ ) or lost ( $\delta U < 0$ ) during the tunneling process [39];  $n_l(E) = |\text{Re}[(E + i\gamma)/\sqrt{(E + i\gamma)^2 - \Delta_l^2(T_l)}]|$  is the (smeared by nonzero  $\gamma \ll \Delta_l$ ) BCS DOS of the  $l = \text{is}, L$ , and  $R$  elements [41]; and  $f_l(E)$  is the Fermi-Dirac distribution function at temperature  $T_l$ . We assumed the SC island to be in equilibrium at temperature  $T_{\text{is}}$ .

In the following, we assume for the physical parameters of the transistor a realistic design [42] for Al-based tunnel structures. The leads are realized with Al ( $\Delta = 220 \mu\text{eV}$ ,  $T_C = 1.2 \text{ K}$ ), whereas the SC island is realized with a Al/Cu bilayer ( $\Delta_{\text{is}} = \Delta/2$ ) with a charging energy  $E_c = 4\Delta$ . The barriers are chosen to be identical ( $R = 1 \text{ M}\Omega$ ) and the temperature gradient can be achieved via Joule heaters localized in the leads.

**Strong violation of detail balance.** The electron tunneling rate from the lead to the island as a function of the electrostatic energy difference  $\delta U$  contains the crucial physics for the bipolar thermoelectric effect, and it is shown in Fig. 1(b) for different temperatures  $T_{\text{hot}}$ . At equilibrium,  $T_{\text{hot}} = T_{\text{cold}}$  (dark blue line), we notice a small peak at  $\delta U^* = \Delta - \Delta_{\text{is}} > 0$ , which corresponds to the matching of the DOS divergences of the two different superconductors, which is activated by the temperature, since at zero temperature it is completely Pauli blocked. At finite temperature in equilibrium, the rates satisfy the detail balance  $\Gamma(-\delta U) = e^{-\delta U/k_B T} \Gamma(\delta U)$ , so correspondingly we expect a small peak [although not visible in Fig. 1(b)] to exist at negative energies  $\delta U = -\delta U^*$  as well.

More intriguing physics arises under out-of-equilibrium conditions. By increasing the lead temperature,  $T_{\text{hot}} > T_{\text{cold}}$ , the peak at negative energy emerges and surpasses its counterpart at positive energy (brown line). This is an unusual situation where  $\Gamma(-|\delta U|) > \Gamma(|\delta U|)$ , and we identify it as a *strong violation of the detail balance*. It comes out as

a consequence of a finite temperature difference populating more states at higher energy in the hot leads. From Eq. (1) a strong violation is possible *only if* for some energy  $\epsilon$ ,  $\delta U > 0$  we have

$$n_{\text{is}}(\epsilon - \delta U)[1 - f_{\text{is}}(\epsilon - \delta U)] > n_{\text{is}}(\epsilon + \delta U) \times [1 - f_{\text{is}}(\epsilon + \delta U)]. \quad (2)$$

This inequality constitutes a *necessary* condition and it depends only on the island DOS and on its Fermi function. It can be shown [43] that Eq. (2) is meaningful *only if* there is a gap asymmetry between the hot and cold sides, and the superconducting DOS features a monotonously decreasing energy dependence for  $|E| > \Delta$  [32]. Furthermore, in order to be satisfied, Eq. (2) *implicitly* requires that the BCS island DOS shifts with the electrochemical potential (the electrostatic energy difference  $\delta U$  in the rate). Indeed, if the DOS does not depend on  $\delta U$  [i.e., substituting  $n_{\text{is}}(\epsilon \pm \delta U) \rightarrow n_{\text{is}}(\epsilon)$  like in a semiconductor], Eq. (2) cannot be satisfied since  $n_{\text{is}} > 0$ . Thus, the strong violation stems essentially from the interacting character captured by the BCS mean-field theory and, as we are going to show, it is the essential precursor of the bipolar thermoelectric phenomena. The fundamental role of the interaction clarifies also well why this effect can be associated with a spontaneous symmetry breaking of the EH symmetry induced by the out-of-equilibrium condition [32,34,35]. In fact, the capability of the BCS DOS to rigidly shift with the electrochemical potential, together with its monotonic decreasing nature for  $|E| > \Delta$ , leads to a system that transports electrons and holes in a different way, without an explicit breaking of the spectral EH symmetry for the DOS. Intriguingly, a suitable temperature gradient leads to a thermocurrent against the bias (absolute negative conductance).

**Current.** In the sequential tunneling approximation we get the electric current through a standard master equation approach [44–46], in which the time evolution of the population  $P_n$  of the island charge state  $n$  is determined by  $\dot{P}_n = \sum_{n'} \mathbf{W}_{nn'} P_{n'}$ . The kernel  $\mathbf{W}_{nn'} = \sum_{j=R,L} \Gamma_j^{nn'}$ , with the diagonal terms  $\mathbf{W}_{nn}$  fixed by the conservation of the probability,  $\sum_n P_n = 1$ , implying  $\sum_n \mathbf{W}_{nn'} = 0$ . The rates  $\Gamma_j^{n,n\pm 1} = \Gamma_j(\delta U_{n,n\pm 1})$  correspond only to the transitions  $n = n' \pm 1$  described by the rates of Eq. (1). The electrostatic energy differences are  $\delta U_{n,n\pm 1} = U(n \pm 1) - U(n) \pm eV/2$  following the usual form of the “orthodox” theory [39,44,47], with  $V = V_L - V_R$  being the source-drain bias and  $U(n) = E_C(n - q_{\text{is}}/e)^2/2$  the electrostatic energy. This depends on the offset charge on the island  $q_{\text{is}} = C_g V_g + \sum_j C_j V_j$ , with  $C_g$  being the gate capacitance and  $C_j$  the  $j$ th barrier capacitance (for which  $C_{\text{tot}} = C_g + C_L + C_R$ ). In the stationary limit [47], the current can be simply computed in the right lead  $I = I_R = -I_L = e \sum_n [\Gamma_R^{n,n+1} - \Gamma_R^{n,n-1}] P_n^0$ , where  $P_n^0$  is the stationary probability of island charge states. This general numerical approach can be further simplified in the Coulomb blockade regime  $k_B T \ll E_C$  by noting that the dominant contribution to the transport at one resonance is associated only with the tunneling rates involving neighboring charge states  $n - 1 \rightleftharpoons n$ . The current in such a case can be written as

$$I_n = e \frac{\Gamma_L^f(n-1)\Gamma_R^f(n) - \Gamma_L^b(n)\Gamma_R^b(n-1)}{\Gamma_L^f(n-1) + \Gamma_R^f(n) + \Gamma_L^b(n) + \Gamma_R^b(n-1)}, \quad (3)$$

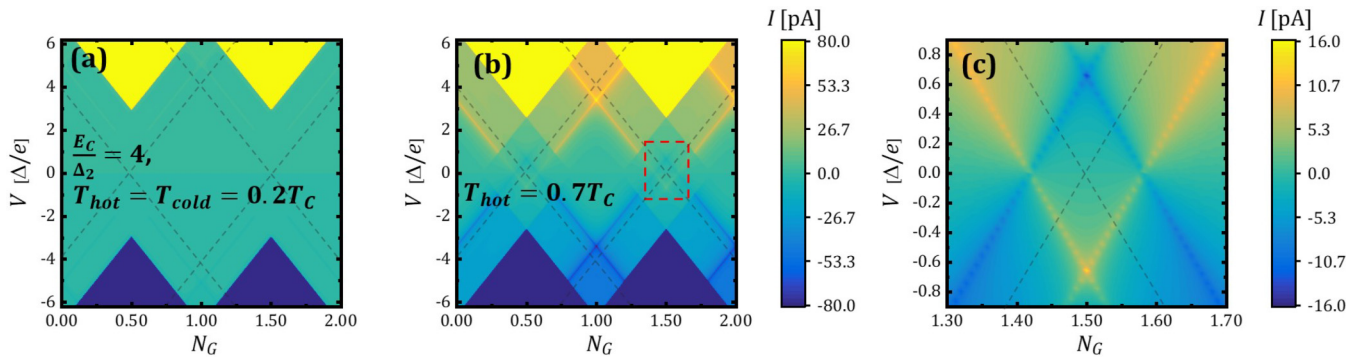


FIG. 2. (a), (b) Charge current flowing through the  $SIS'IS$  structure at thermal equilibrium (a) and in the nonlinear regime (b) vs  $V$  and  $N_G = C_g V_G/e$ . The color scale is the same for both graphs. (c) Blow-up of the red-dashed region shown in panel (b) where the onset of the thermoelectric behavior is clearly visible. The calculation parameters are the same as those in Fig. 1.

where we use a shortened notation for the rates  $\Gamma_j^{f/b}(n) = \Gamma_j(\pm \delta U_{n,n\pm 1})$ . Since we are mainly interested in the deep subgap regime in the bias range  $|eV| < 2\Delta$  with  $E_C = 4\Delta$ , we approximate the current by considering the dominant contribution of two neighboring Coulomb resonances, i.e.,  $I = I_n + I_{n+1} + \mathcal{O}(e^{-E_C/2k_B T_{\text{hot}}})$ .

**Coulomb diamonds.** Figures 2(a) and 2(b) show the current  $I$  as a function of the source-drain bias  $V$  and the gate-tunable offset charge  $N_G = C_g V_G/e$ . Typical Coulomb diamonds appear, which display periodicity in the offset charge  $N_G$  in units of the electron charge  $e$ . The system does not present any even-odd effect since the average Cooper pair recombination rate in our system  $\Gamma_r \simeq 16$  kHz [42] is much smaller than the tunneling rates  $\Gamma_j \sim I/e$  (inverse average electron dwelling time in the island). Coulomb diamonds at equilibrium are shown in Fig. 2(a). As a guide for the eye, we show with black dashed lines the boundaries of the Coulomb diamonds for  $\Delta = 0$ , where the electrostatic energies vanish,  $\delta U_{n,n\pm 1}(N_G, V) \equiv 0$ . As expected, the SC gap pushes the boundaries of the Coulomb diamonds up in energy, and charge transport is suppressed in the  $(N_G, V)$  plane domains satisfying  $(eV < 2\Delta + 2\Delta_{is} \approx 3\Delta)$ .

Figure 2(b) shows the results for the nonequilibrium case,  $T_{\text{hot}} = 0.7 T_C > T_{\text{cold}}$ . Subgap conduction channels become visible, as thermally excited states promote the stronger emergence of the matching peak resonances. At integer  $N_G$  and  $|eV| \sim 3\Delta$ , where the transport is dissipative ( $IV > 0$ ) even if fully inside the Coulomb blockade diamond, we clearly see the appearance of yellow (blue) crosses at positive (negative)  $V$ . These features stem from the enhancement of the *negative energy* peak in the tunneling rate for electrostatic energy  $\delta U \approx -\delta U^*$  [see Fig. 1(b)] and are also a direct consequence of the strong violation of the detailed balance, even if their nature is still dissipative. More intriguingly, for half-integer  $N_G$  and  $eV \sim \Delta/2$ , the sign of the current becomes opposite to the bias  $IV < 0$ , as shown in the blow-up of Fig. 2(c). This behavior is a signature of thermoelectricity and it appears *only* when a finite temperature difference is applied between the island and the hot leads. These subgap structures are equivalently present at positive and negative bias for the *same* temperature difference, showing the full *bipolar* character that is enforced by the spectral EH symmetry of the unbiased system. The emerging bipolar thermoelectric effect

is similar to  $SIS'$  systems [33]. Furthermore, our bipolar thermoelectric superconducting transistor offers the possibility to be manipulated thanks to Coulomb interaction and associated gating effects. We stress that, unlike a conventional quantum-dot thermoelectric effect [48,49] that is activated by a temperature gradient *between* the leads, the present effect appears when the leads have the *same* temperature higher than the Coulomb island [43].

Figure 3(a) displays cuts of Fig. 2(b) at different values of  $V$ . In a region around the half-integer gate charge  $N_G$  we clearly see a change of the sign of the current around the Coulomb resonance opposite to the bias (thermoelectric effect). Notably, the sign of the thermoelectric current does not change passing through the resonant value due to the unique bipolar nature, unlike in the conventional (unipolar) thermoelectric effect in a quantum dot [25]. Figure 3(b) shows cuts

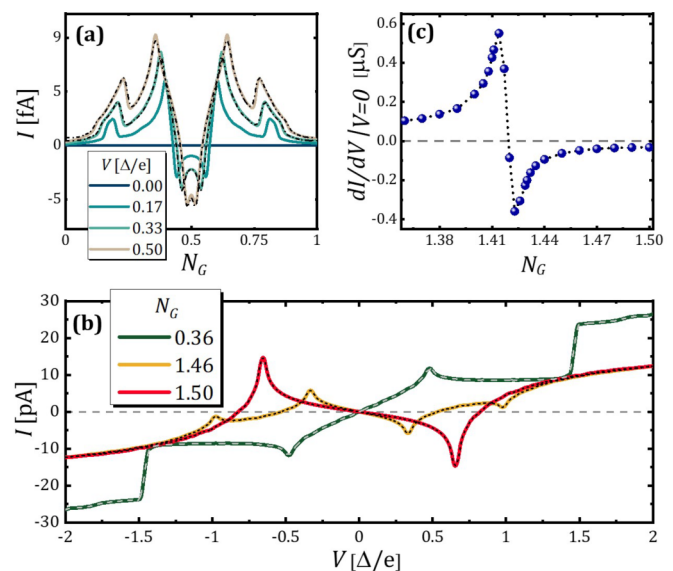


FIG. 3. Out-of-equilibrium ( $T_{\text{hot}} = 0.7 T_C$ ) current  $I$  vs (a)  $N_G$  for different values of  $V$  and (b)  $V$  for different values of  $N_G$  [respectively, horizontal and vertical cuts of Fig. 2(b)]. Dashed lines correspond to the prediction of the simplified model Eq. (3), showing its validity in the case of  $E_C \gg eV$ . (c) Out-of-equilibrium zero-bias conductance vs  $N_G$  calculated for the curves in panels (b).

of Fig. 2(b) at fixed  $N_G$ . We first focus on the zero-bias behavior: as we vary  $N_G$  towards half-integer values the zero-bias conductance (ZBC)  $G_0 = dI/dV|_{V=0}$  becomes negative at the critical value  $N_G^* \approx 1.42$  [see Fig. 3(c)]. This behavior blatantly suggests the spontaneous breaking of the EH symmetry of the system [32,33] and highlights the unique capability of the gate control in our system that, differently from other platforms [36], allows one to continuously tune the bipolar thermoelectric properties. A negative ZBC, together with the condition  $I(0, \Delta T) = 0$  as dictated by spectral EH symmetry, implies the existence of thermoelectricity ( $IV < 0$ ) and the existence of a Seebeck voltage  $V_S$ , since at high-biases  $eV \gg 3\Delta$  the system necessarily becomes again dissipative,  $IV > 0$ . Interestingly, this implies that the Seebeck voltage (i.e., open circuit voltage defined as  $I(V_S) = 0$ ) is expected to be dependent on the gate voltage,  $V_S(N_G)$ , with clear consequences on the gate tunability of the thermoelectric performance. At finite values of  $V$  the current exhibits a peak changing in sign (thermoelectricity) when  $N_G$  approaches half-integer values. The system shows an absolute negative conductance and thereby thermopower,  $\tilde{W} = -IV > 0$ . Furthermore, for some values of  $N_G$  the  $IV$  curve presents more than one resonant peak (see yellow line): this is a consequence of the Coulomb blockade, since the island electrostatic energy differences  $\delta U$  for different rates depend on the gate  $N_G$  and the bias  $V$ , and correspondingly the matching peaks resonance of the dominant rates appear split for nonresonant values  $N_G \neq 1/2 + n$  of the  $IV$  curve. Note that a similar double-peak structure can be observed also as a function of  $N_G$ , as shown in Fig. 3(b).

**Thermoelectric figures of merit.** The intrinsic nonlinear nature of the above effect does not allow us to describe the thermoelectric figures of merit of our system via a linear thermoelectric approach [50]. However, we can still define a Seebeck voltage  $V_S$  and a nonlinear Seebeck coefficient  $\mathcal{S} = V_S/\Delta T$ , with  $\Delta T = T_{\text{hot}} - T_{\text{cold}}$ . We stress that spectral EH symmetry implies two Seebeck voltages,  $\pm V_S$ , and a *bipolar*  $\mathcal{S}$  [32]. Figure 4(a) shows  $V_S$  (solid line, left scale) and  $|\mathcal{S}|$  (dashed line, right scale) as a function of  $N_G$  for different temperatures of the leads. By changing  $T_{\text{hot}}$ , the Seebeck voltage shows hornlike nonlinear features which are even higher at slightly lower values of  $T_{\text{hot}}$ . By inspection of Fig. 3(b) we recognize that the yellow curve has two peaks and for certain values of  $\Delta T$  the second peak can even cross the  $I = 0$  axis, returning a higher open circuit (Seebeck) voltage. Analogously,  $\mathcal{S}$  is also similarly affected and its maximal value is not necessarily associated to the maximal thermovoltage (due to the nonlinearities it is not even necessarily associated with the highest temperature difference  $\Delta T$ ). In Fig. 4(b) the maximum thermocurrent  $I_{\text{max}}(N_G) = \max_{0 < V < 2\Delta/e} [I(V, N_G)]$  as a function of  $N_G$  is shown to gradually become zero while lowering  $T_{\text{hot}}$ , as expected, since the temperature difference is not enough to trigger the bipolar thermoelectricity [34,35]. The thermoelectric generator character of the transistor appears when closing the circuit on a load resistor. Figure 4(c) displays the output power of the structure as a function of  $N_G$  for different values of the load resistor, demonstrating the ability of fine gating control of the output power. The maximum achievable

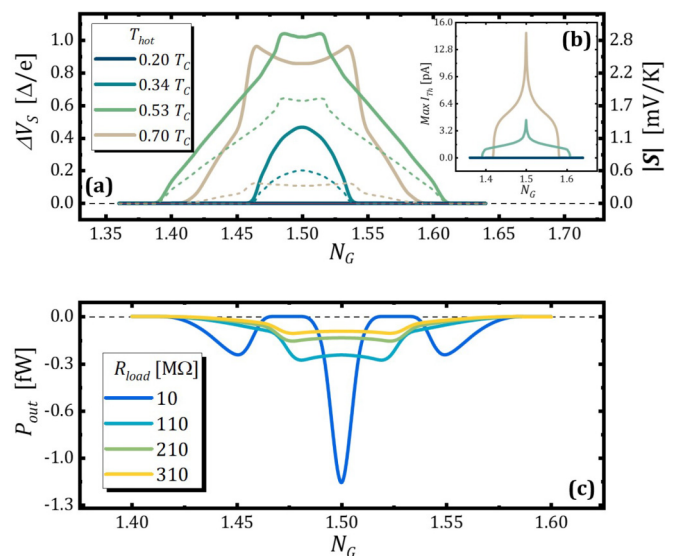


FIG. 4. (a) Seebeck voltage (left y axis) and nonlinear Seebeck coefficient  $|\mathcal{S}|$  (right y axis) vs  $N_G$  for different values of  $T_{\text{hot}}$ . (b) Maximum thermocurrent vs  $N_G$  for different values of  $T_{\text{hot}}$ . (c) Power output  $P_{\text{out}} = -\tilde{I}\tilde{V}$  vs  $N_G$  for a few values of the load resistor.  $\tilde{I}$  and  $\tilde{V}$  are the solutions of the intersection of the  $IV$  characteristics with the load line of the resistor. Among all possible solutions only that with  $dI/dV > 0$  can be operated by the engine [32,38].

output power is typically associated with the smallest possible load resistance and turns out to depend on several parameters.

**Conclusions.** We theoretically proposed and analyzed a bipolar thermoelectric superconducting single-electron transistor that enables tuning and control of the bipolar thermoelectric effect through an applied gate voltage. The interplay between Coulomb blockade and out-of-equilibrium thermoelectricity finds its origin in the strong violation of the detail balance, which is triggered by different SC gaps, by a finite temperature difference, and, crucially, by the interacting nature intrinsic to superconductivity. We investigated the performance of a fully gate-tunable heat engine that can provide, with realistic parameters, a nonlinear Seebeck coefficient up to  $\sim 3$  mV/K at subKelvin temperatures. The effect can be implemented in a structure that can produce gate-controlled single-electron thermoelectricity in a fully superconducting design, thereby fostering interest on on-chip energy harvesting and management, single-charge electronics, and single-photon detection [37].

**Acknowledgments.** We acknowledge the EU's Horizon 2020 Research and Innovation Framework Programme under Grants No. 964398 (SUPERGATE) and No. 101057977 (SPECTRUM) and the PNRR MUR project (Grant No. PE0000023-NQSTI) for partial financial support. A.B. acknowledges the PRIN2022 PNRR MUR project NETheQS (Grant No. 2022B9P8LN) and the Royal Society through the International Exchanges between the UK and Italy (Grant No. IEC R2 192166.) for partial financial support.

- [1] G. Benenti, G. Casati, K. Saito, and R. S. Whitney, Fundamental aspects of steady-state conversion of heat to work at the nanoscale, *Phys. Rep.* **694**, 1 (2017).
- [2] Y. Dubi and M. Di Ventra, Colloquium: Heat flow and thermoelectricity in atomic and molecular junctions, *Rev. Mod. Phys.* **83**, 131 (2011).
- [3] R. Kosloff, Quantum thermodynamics: A dynamical viewpoint, *Entropy* **15**, 2100 (2013).
- [4] U. Seifert, Stochastic thermodynamics, fluctuation theorems and molecular machines, *Rep. Prog. Phys.* **75**, 126001 (2012).
- [5] M. Campisi, P. Hanggi, and P. Talkner, Colloquium: Quantum fluctuation relations: Foundations and applications, *Rev. Mod. Phys.* **83**, 771 (2011).
- [6] F. Giazotto, T. T. Heikkilä, A. Luukanen, A. M. Savin, and J. P. Pekola, Opportunities for mesoscopics in thermometry and refrigeration: Physics and applications, *Rev. Mod. Phys.* **78**, 217 (2006).
- [7] A. Fornieri and F. Giazotto, Towards phase-coherent caloritronics in superconducting circuits, *Nat. Nanotechnol.* **12**, 944 (2017).
- [8] J. T. Muhonen, M. Meschke, and J. P. Pekola, Micrometre-scale refrigerators, *Rep. Prog. Phys.* **75**, 046501 (2012).
- [9] N. Brunner, N. Linden, S. Popescu, and P. Skrzypczyk, Virtual qubits, virtual temperatures, and the foundations of thermodynamics, *Phys. Rev. E* **85**, 051117 (2012).
- [10] A. C. Barato and U. Seifert, Thermodynamic uncertainty relation for biomolecular processes, *Phys. Rev. Lett.* **114**, 158101 (2015).
- [11] M. Polettini, G. Verley, and M. Esposito, Efficiency statistics at all times: Carnot limit at finite power, *Phys. Rev. Lett.* **114**, 050601 (2015).
- [12] G. Verley, M. Esposito, T. Willaert, and C. Van den Broeck, The unlikely Carnot efficiency, *Nat. Commun.* **5**, 4721 (2014).
- [13] P. Pietzonka and U. Seifert, Universal trade-off between power, efficiency, and constancy in steady-state heat engines, *Phys. Rev. Lett.* **120**, 190602 (2018).
- [14] S. K. Manikandan, L. Dabelow, R. Eichhorn, and S. Krishnamurthy, Efficiency fluctuations in microscopic machines, *Phys. Rev. Lett.* **122**, 140601 (2019).
- [15] J. P. Pekola, F. Giazotto, and O.-P. Saira, Radio-frequency single-electron refrigerator, *Phys. Rev. Lett.* **98**, 037201 (2007).
- [16] O.-P. Saira, M. Meschke, F. Giazotto, A. M. Savin, M. Möttönen, and J. P. Pekola, Heat transistor: Demonstration of gate-controlled electronic refrigeration, *Phys. Rev. Lett.* **99**, 027203 (2007).
- [17] A. Fornieri, M. J. Martínez-Pérez, and F. Giazotto, A normal metal tunnel-junction heat diode, *Appl. Phys. Lett.* **104**, 183108 (2014).
- [18] S. Tirelli, A. M. Savin, C. P. Garcia, J. P. Pekola, F. Beltram, and F. Giazotto, Manipulation and generation of supercurrent in out-of-equilibrium Josephson tunnel nanojunctions, *Phys. Rev. Lett.* **101**, 077004 (2008).
- [19] B. Sothmann, F. Giazotto, and E. M. Hankiewicz, High-efficiency thermal switch based on topological Josephson junctions, *New J. Phys.* **19**, 023056 (2017).
- [20] N. R. Claughton and C. J. Lambert, Thermoelectric properties of mesoscopic superconductors, *Phys. Rev. B* **53**, 6605 (1996).
- [21] A. Ozaeta, P. Virtanen, F. S. Bergeret, and T. T. Heikkilä, Predicted very large thermoelectric effect in ferromagnet-superconductor junctions in the presence of a spin-splitting magnetic field, *Phys. Rev. Lett.* **112**, 057001 (2014).
- [22] F. Vischi, M. Carrega, P. Virtanen, E. Strambini, A. Braggio, and F. Giazotto, Thermodynamic cycles in Josephson junctions, *Sci. Rep.* **9**, 3238 (2019).
- [23] G. Marchegiani, P. Virtanen, F. Giazotto, and M. Campisi, Self-oscillating Josephson quantum heat engine, *Phys. Rev. Appl.* **6**, 054014 (2016).
- [24] K. Brandner, K. Saito, and U. Seifert, Strong bounds on Onsager coefficients and efficiency for three-terminal thermoelectric transport in a magnetic field, *Phys. Rev. Lett.* **110**, 070603 (2013).
- [25] B. Sothmann, R. Sánchez, and A. N. Jordan, Thermoelectric energy harvesting with quantum dots, *Nanotechnology* **26**, 032001 (2015).
- [26] M. Esposito, K. Lindenberg, and C. V. den Broeck, Thermoelectric efficiency at maximum power in a quantum dot, *Europhys. Lett.* **85**, 60010 (2009).
- [27] R. S. Whitney, Most efficient quantum thermoelectric at finite power output, *Phys. Rev. Lett.* **112**, 130601 (2014).
- [28] F. Ronetti, L. Vannucci, G. Dolcetto, M. Carrega, and M. Sasseti, Spin-thermoelectric transport induced by interactions and spin-flip processes in two-dimensional topological insulators, *Phys. Rev. B* **93**, 165414 (2016).
- [29] M. Kamp and B. Sothmann, Phase-dependent heat and charge transport through superconductor-quantum dot hybrids, *Phys. Rev. B* **99**, 045428 (2019).
- [30] R. Hussein, M. Governale, S. Kohler, W. Belzig, F. Giazotto, and A. Braggio, Nonlocal thermoelectricity in a Cooper-pair splitter, *Phys. Rev. B* **99**, 075429 (2019).
- [31] N. F. Mott, H. Jones, H. Jones, and H. Jones, *The Theory of the Properties of Metals and Alloys* (Dover, Mineola, New York, 1958).
- [32] G. Marchegiani, A. Braggio, and F. Giazotto, Nonlinear thermoelectricity with electron-hole symmetric systems, *Phys. Rev. Lett.* **124**, 106801 (2020).
- [33] G. Marchegiani, A. Braggio, and F. Giazotto, Superconducting nonlinear thermoelectric heat engine, *Phys. Rev. B* **101**, 214509 (2020).
- [34] G. Germanese, F. Paolucci, G. Marchegiani, A. Braggio, and F. Giazotto, Bipolar thermoelectric Josephson engine, *Nat. Nanotechnol.* **17**, 1084 (2022).
- [35] G. Germanese, F. Paolucci, G. Marchegiani, A. Braggio, and F. Giazotto, Phase control of bipolar thermoelectricity in Josephson tunnel junctions, *Phys. Rev. Appl.* **19**, 014074 (2023).
- [36] L. Bernazzani, G. Marchegiani, F. Giazotto, S. Roddaro, and A. Braggio, Bipolar thermoelectricity in bilayer-graphene-superconductor tunnel junctions, *Phys. Rev. Appl.* **19**, 044017 (2023).
- [37] F. Paolucci, G. Germanese, A. Braggio, and F. Giazotto, A highly sensitive broadband superconducting thermoelectric single-photon detector, *Appl. Phys. Lett.* **122**, 173503 (2023).
- [38] G. Marchegiani, A. Braggio, and F. Giazotto, Phase-tunable thermoelectricity in a Josephson junction, *Phys. Rev. Res.* **2**, 043091 (2020).
- [39] D. Averin and K. Likharev, Single electronics: A correlated transfer of single electrons and Cooper pairs in systems of small tunnel junctions, in *Modern Problems in Condensed Matter Sciences* (Elsevier, Amsterdam, 1991), Vol. 30, pp. 173–271.

- [40] J. P. Pekola, J. J. Vartiainen, M. Möttönen, O.-P. Saira, M. Meschke, and D. V. Averin, Hybrid single-electron transistor as a source of quantized electric current, *Nat. Phys.* **4**, 120 (2008).
- [41] R. C. Dynes, J. P. Garno, G. B. Hertel, and T. P. Orlando, Tunneling study of superconductivity near the metal-insulator transition, *Phys. Rev. Lett.* **53**, 2437 (1984).
- [42] V. F. Maisi, S. V. Lotkhov, A. Kemppinen, A. Heimes, J. T. Muhonen, and J. P. Pekola, Excitation of single quasiparticles in a small superconducting Al island connected to normal-metal leads by tunnel junctions, *Phys. Rev. Lett.* **111**, 147001 (2013).
- [43] See Supplemental Material at <http://link.aps.org/supplemental/10.1103/PhysRevResearch.6.L012022> for a derivation of necessary and sufficient conditions for the bipolar thermoelectric effect to arise, and for a detailed discussion on the analogies and differences between this effect and the conventional one.
- [44] Y. V. Nazarov and Y. M. Blanter, *Quantum Transport: Introduction to Nanoscience* (Cambridge University Press, Cambridge, 2009).
- [45] D. A. Bagrets and Y. V. Nazarov, Full counting statistics of charge transfer in Coulomb blockade systems, *Phys. Rev. B* **67**, 085316 (2003).
- [46] A. Braggio, J. König, and R. Fazio, Full counting statistics in strongly interacting systems: Non-Markovian effects, *Phys. Rev. Lett.* **96**, 026805 (2006).
- [47] C. W. J. Beenakker, Theory of Coulomb-blockade oscillations in the conductance of a quantum dot, *Phys. Rev. B* **44**, 1646 (1991).
- [48] A. A. M. Staring, L. W. Molenkamp, B. W. Alphenaar, H. van Houten, O. J. A. Buyk, M. A. A. Mabeoone, C. W. J. Beenakker, and C. T. Foxon, Coulomb-blockade oscillations in the thermopower of a quantum dot, *Europhys. Lett.* **22**, 57 (1993).
- [49] G. D. Mahan and J. O. Sofo, The best thermoelectric, *Proc. Natl. Acad. Sci. USA* **93**, 7436 (1996).
- [50] H. Goldsmid, *Thermoelectric Refrigeration* (Springer, Berlin, 2013).